

Review

Advancements, Challenges and Prospects of Chemical Vapour Pressure at Atmospheric Pressure on Vanadium Dioxide Structures

Charalampos Drosos ¹  and Dimitra Vernardou ^{2,3,*} 

¹ Delta Nano-Engineering Solutions Ltd., Paddock Wood, Kent TN12 6EL, UK; info@delta-nano.com

² Center of Materials Technology and Photonics, School of Applied Technology, Technological Educational Institute of Crete, 710 04 Heraklion, Crete, Greece

³ Institute of Electronic Structure and Laser, Foundation for Research & Technology-Hellas, P.O. Box 1527, Vassilika Vouton, 711 10 Heraklion, Crete, Greece

* Correspondence: dimitra@iesl.forth.gr; Tel.: +30-2810-379-774

Received: 1 February 2018; Accepted: 27 February 2018; Published: 5 March 2018

Abstract: Vanadium (IV) oxide (VO₂) layers have received extensive interest for applications in smart windows to batteries and gas sensors due to the multi-phases of the oxide. Among the methods utilized for their growth, chemical vapour deposition is a technology that is proven to be industrially competitive because of its simplicity when performed at atmospheric pressure (APCVD). APCVD's success has shown that it is possible to create tough and stable materials in which their stoichiometry may be precisely controlled. Initially, we give a brief overview of the basic processes taking place during this procedure. Then, we present recent progress on experimental procedures for isolating different polymorphs of VO₂. We outline emerging techniques and processes that yield in optimum characteristics for potentially useful layers. Finally, we discuss the possibility to grow 2D VO₂ by APCVD.

Keywords: APCVD; VO₂; processing parameters; 2D

1. Chemical Vapour Deposition

1.1. General Information

CVD is a practical method of atomistic or near atomistic deposition having the ability to synthesize well-controlled dimensions and structures at reasonably low temperatures, high purity and in multiple formats such as single layer, multi-layer, composite and finally functional coatings. In its simplest incarnation, CVD encompasses a single precursor gas flowing into a chamber containing the substrate to be coated. Although, there are exceptions, the vapour of the reactive compound, usually an easily volatilized liquid or in some cases a solid, is sublimed directly and transported to the reaction zone by a carrier gas. A thin film is then deposited by chemical reaction or decomposition of the gas mixture on the substrate surface or in its vicinity at a defined temperature.

The precursors used within a variety of CVD techniques can be single source or dual source in origin. Single source precursors contain all the groups/elements required for successive thin film production. On the other hand, dual source precursors involve the interaction between multiple precursors for the synthesis of thin films. In each case, it is vital for production of thin films to deliver the gas phase precursors with a carrier gas. The most common carrier gases are N₂, He or Ar, especially when highly reactive or pyrophoric reactants are used and in some cases, reactions entail an energy input from the carrier gas, e.g., H₂ or O₂ enrichment.

Reactor systems in CVD processes must allow controlled transport of the reactant and diluent gases to the reaction zone, maintain a defined substrate temperature and safely remove the gaseous

by-products. These functions should be fulfilled with sufficient control and maximal effectiveness, which requires optimum engineering design and automation. The reactor in which the thin film deposition actually takes place is the essential part of the system and must be designed according to the specific chemical process parameters. To coat layers using Chemical Vapour Deposition at Atmospheric Pressure (APCVD), four basic types can be classified according to their gas flow and operation principles:

1. Horizontal tube displacement flow type.
2. Rotary vertical batch type.
3. Continuous—deposition type using premixed gas flow.
4. Continuous—deposition type employing separate gas streams.

1.2. CVD Processes

Any CVD process including APCVD involves the subsequent operations. First, the reacting gas is directed into the reactor. The gas moves towards its thermal equilibrium temperature and composition through gas-phase collisions and reactions. Near-equilibrated species are then transported to the reaction surface, the surface chemical reactions commence and the thin film is formed. The processes are summarized below (Figure 1) [1]:

1. Creation of active gaseous reactants.
2. Transport of the precursor to the CVD reactor.
3. Decomposition of gas phase precursor to remove gaseous by-products and grow reactive intermediates.
4. Gaseous reactants transportation onto substrate area.
5. Surface diffusion for nucleation and thin film growth.
6. Desorption of by-products and mass transport away from active reactive zone.

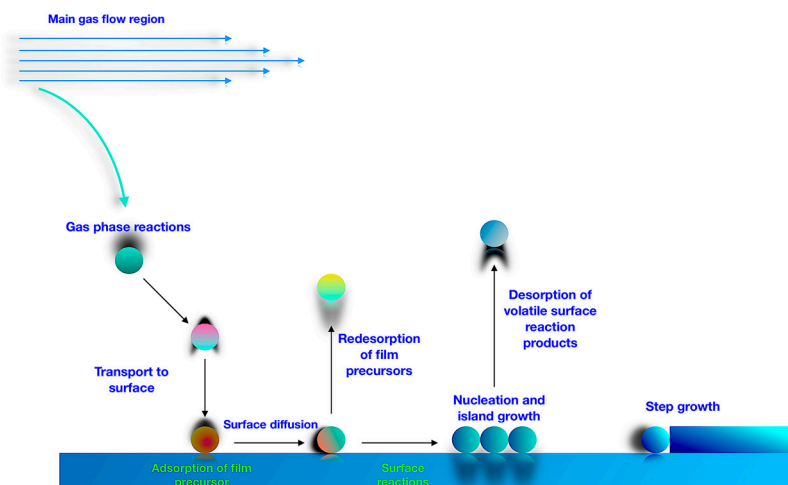


Figure 1. Schematic view of CVD (Chemical Vapour Deposition) process [1].

1.3. APCVD

A schematic presentation of the APCVD system is shown in Figure 2. It is designed with no joints in all outlet lines to avoid blocking. A flow of inert gas, usually nitrogen, is passed through the apparatus during all operations. The amount of the precursor delivered into the reactor is calculated from the Equation (1)

$$a = \frac{VP \times F}{(760 - VP) \times 24.4} \quad (1)$$

where a , is the amount of precursor (mol min^{-1}), VP , is the vapour pressure of precursor at the bubbler's temperature (mm Hg), F , is the nitrogen flow rate through the bubbler (L min^{-1}) and 24.4, is a constant for the molar volume of an ideal gas at standard temperature and pressure (L mol^{-1}).

In a typical APCVD experiment, once all temperatures are stabilized over time, the N_2 is passed through the bubblers and then the precursor gas flow rate is directed into the mixing chamber where the mixture begins in order to be utilized before entering the reaction chamber for the deposition to take place. Once the allotted time is complete, the precursor bubbler is closed. The reactor heater is turned off and the substrate is allowed to cool down under an atmosphere of N_2 . Ideally, the carrier gas inlet flows should be fully saturated with precursor vapour; this can be achieved with knowledge of the precursor volatility and vapour pressure and then controlled by the carrier gas flow and bubbler temperature using flow meters and heating jackets.

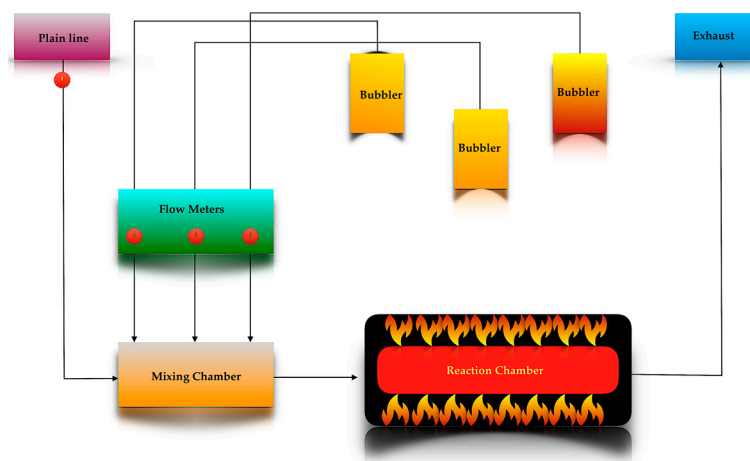


Figure 2. Schematic presentation of an APCVD (Chemical Vapour Deposition at Atmospheric Pressure) system [1].

2. Vanadium Oxides

The binary Vanadium-Oxygen phase diagram consists of a large number of phases between V_2O_3 and VO_2 of the form $\text{V}_n\text{O}_{2n-1}$ commonly known as the Magneli phases [2] that exhibit distinctive electrical and optical properties. The variety of Vanadium-Oxygen stoichiometries emerges from the ability of vanadium atoms to adopt multiple oxidation states, which consequently results in synthetic challenges to control the structure of the materials [3].

More than ten kinds of crystalline phases of VO_2 have been reported elsewhere, whereas some examples are monoclinic VO_2 (M), tetragonal VO_2 (R) and several metastable forms of VO_2 (A), VO_2 (B) and VO_2 (C) [4]. Among these phases, only the rutile VO_2 (R/M) phase undergoes a fully reversible metal insulator transition at a critical temperature (T_c) [1], where an abrupt alteration in optical and electronic properties is observed making it ideal for optoelectronic switches [5], memristors [6], artificial neuron networks [7,8] and intelligent window coatings [9,10].

The high temperature phase ($T > T_c$), has a tetragonal type structure characterized by chains of edge sharing $[\text{VO}_6]$ octahedral along the c -axis with equidistant vanadium atoms ($V-V = 2.88 \text{ \AA}$) [11]. While, the low temperature structure involves $\text{V}^{4+}-\text{V}^{4+}$ pairing with alternate shorter (0.265 nm) and longer (0.312 nm) $\text{V}^{4+}-\text{V}^{4+}$ distances along the a -axis and tilting with respect to the rutile c -axis [11]. At 25 °C, the lattice has unit cell parameters; $a = 5.75 \text{ \AA}$, $b = 4.52 \text{ \AA}$, $c = 5.38 \text{ \AA}$ and $\beta = 122.60^\circ$ [12]. The lattice is the result of the distortion occurring at the high temperature metallic tetragonal phase.

The mechanism of metal insulator transition in VO₂ has been investigated through computational, experimental and theoretical studies [13–15]. Nevertheless, the mechanism of the transition remains unresolved, since the VO₂ phases exhibit diverse lattice structures but have analogous electronic properties.

3. Advancements

There have been numerous studies on the VO₂ grown by APCVD since Maruyama and Ikuta utilized vanadium (III) acetylacetonate (V(acac)₃) as a single-precursor to deposit polycrystalline pure VO₂ films on fused quartz and sapphire single crystals [16]. In this review article, we will focus on the progress taking place during the last four years regarding the control of the processing parameters to isolate the VO₂ phases strengthening the functional properties of APCVD VO₂ layers.

The growth of amorphous pure and tungsten doped VO₂ coatings is possible on SnO₂-precoated glass substrates using vanadyl (V) triisopropoxide (VO(OC₃H₇)₃) as single-precursor [9,10,17,18]. It is interesting to note that the presence of tungsten in the lattice of VO₂ changed the surface morphology to worm-like (Figure 3) from granular structure [9]. This approach has several advantages including the high vapour pressure of the precursor (i.e., decomposition over time and transport of unknown species are prevented). Additionally, the operations are simplified by removing the commonly necessary oxygen source, which is usually provided either in the form of pure gas or from an extra bubbler through H₂O or alcohol. Vanadyl (IV) acetylacetonate (VO(acac)₂) along with propanol, ethanol and O₂ gas as oxygen sources is accomplished to grow VO₂ of different crystalline orientations [19,20]. The *a*-axis textured monoclinic is enhanced with propanol and ethanol, while the 002-oriented single phase V₂ is obtained with O₂ gas possessing grains (*a*-axis coatings) and agglomeration of grains forming rod-like structures (002-oriented phases). On controlling the oxygen gas flow rate (Figure 4), isolated monoclinic and metastable VO₂ phases can also be achieved using VO(acac)₂ as vanadium precursor on flexible [21] and SnO₂-precoated glass substrates [22].

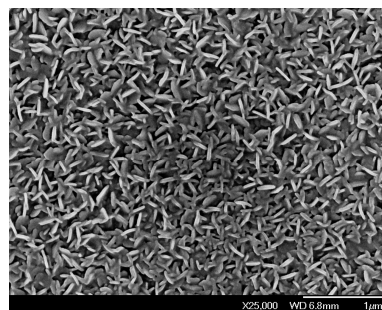


Figure 3. Field emission-scanning electron microscopy image of the APCVD tungsten doped VO₂ coating.

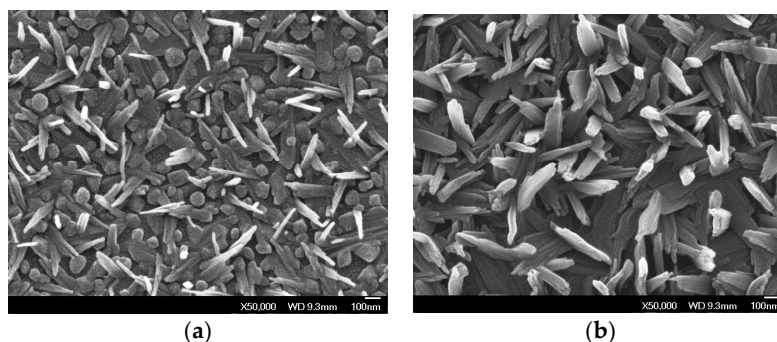


Figure 4. Field emission-scanning electron microscopy images of APCVD vanadium oxides using oxygen flow rate of 0.4 (a) and 0.8 L min^{−1} (b).

SnO_2 was chosen as a substrate due to the similar crystalline structure with VO_2 , which can act as a template for the growth of rutile VO_2 and promote the crystallinity of the oxide [23].

4. Challenges

A comparative study among $\text{VO}(\text{acac})_2$ and VCl_4 , the most utilized vanadium precursors for APCVD VO_2 , indicated that the transport rate of $\text{VO}(\text{acac})_2$ is lower than VCl_4 [24]. This can be handled by increasing the temperature and the N_2 flow rate in the bubbler. However, this is not anticipated because the precursor may decompose over time leading to irreproducible delivery rates and the transport of unknown species. On the other hand, VCl_4 is highly reactive with H_2O resulting in inhomogeneous films [25]. A new approach uses the ethyl acetate (EtAc) as an excellent oxygen precursor resulting in the precise control of the growth rate and porosity of the films after the optimization of VCl_4/EtAc system [26]. A route to improve this system involves the combination of X-ray photoelectron spectroscopy (XPS) and X-ray absorption near-edge structure (XANES) to determine the effect of the substrate choice on the VO_2 formation for functional properties such as thermochromism [27]. It is then possible to grow VO_2 (Figure 5) onto substrates that induce lattice matching (SnO_2) or others (F-doped SnO_2) that promote a destabilization of V^{4+} ions and a further increase in V^{5+} deteriorating the functional properties (Figure 6).

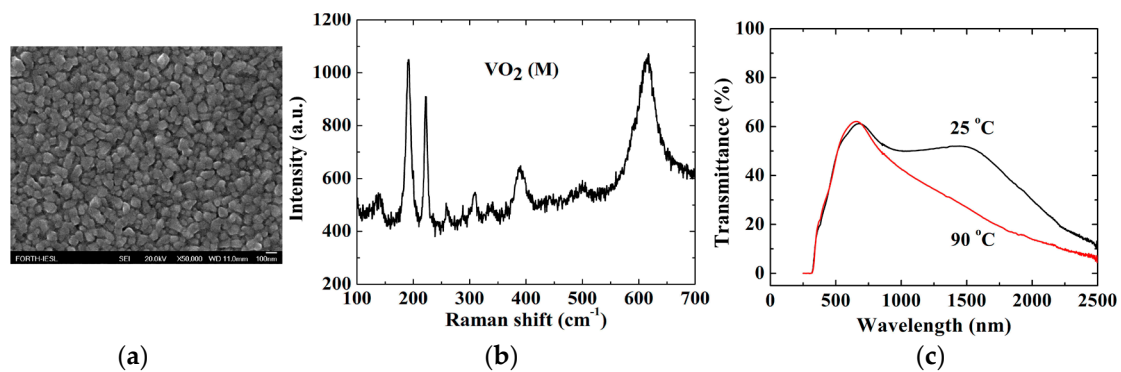


Figure 5. Field emission-scanning electron microscopy image (a) and (b) Raman spectroscopy of APCVD VO_2 grown on SnO_2 -precoated glass substrates. (c) Transmittance spectra below T_c at 25 °C and above T_c at 90 °C over the region of 250–2500 nm to study the thermochromic performance.

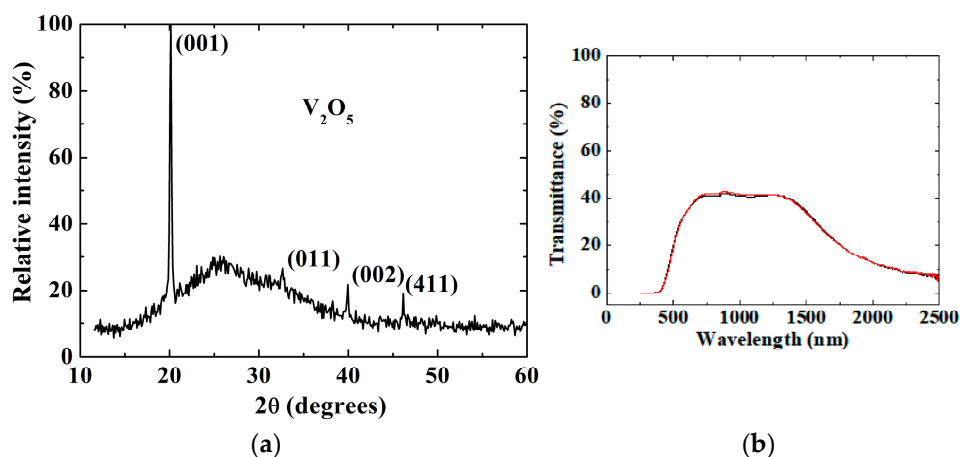


Figure 6. (a) X-ray diffraction of APCVD V_2O_5 grown on F-doped SnO_2 . (b) No change in transmittance spectra observed over the region 250–2500 nm below T_c at 25 °C (black colour) and above T_c at 90 °C (red colour).

Furthermore, monoclinic VO₂ exhibits poor adhesion and is chemically susceptible to attack, restricting the use as solar control coating. In that respect, multi-functional, robust APCVD VO₂/SiO₂/TiO₂ films on glass substrates demonstrates excellent solar modulation properties, high transparency and resistance to abrasion compared to single VO₂ films of the same thickness [28].

5. Prospects and Outlook

In the field of APCVD VO₂, the altering of the processing parameters and the manipulation of the substrate surface is just starting to be understood. New evolvments in experimental procedures such as the utilization of single vanadium precursor and the oxygen source have addressed APCVD routes in isolating the intrinsic material properties. There are numerous exciting challenges in developing VO₂ with functional properties, which expand our understanding of the underlying chemistry and potentially lead to anticipated applications.

Two-dimensional (2D) VO₂ can also be possible by APCVD through Computational Fluid Dynamics (CFD) simulations. CFD simulations are performed to evaluate and define the whole experimental process, before, while and after the experimental procedure isolating the intrinsic material properties (Figure 7). CFD results of exhaust and quartz tube presented the simulation procedure regarding the flow rates and the temperature distribution along the boundaries of the metallic parts. The flow rate of N₂ was set at 0.1 L min⁻¹ and the temperature in the inner boundaries was at 300 °C. Every aspect of the APCVD process is simulated to approach the optimal characteristics of the oxide in tandem to the surface to be deposited. Prospects in developing the growth of high-quality large-area materials with well-defined sizes, high dispersion and excellent control on layer thickness will then appear. The potential impact is illustrated by considering the exploitation possibilities of the high-performance materials by APCVD to create advanced devices for practical applications.

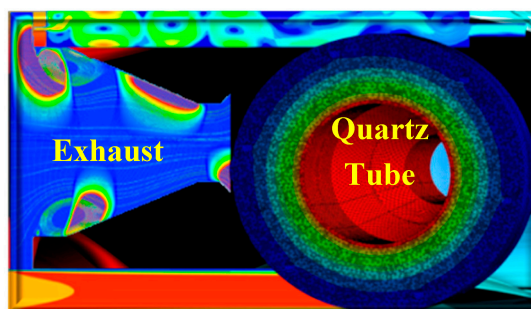


Figure 7. Simulation of transport species within the components of the APCVD reactor. The simulation showed an increase of the fluid's velocity from $2.359 \times 10^{-3} \text{ m s}^{-1}$ to $3.283 \times 10^{-3} \text{ m s}^{-1}$, i.e., an increase of velocity of 39.18% due to temperature change. (Image courtesy of Delta Nano—Engineering Solutions Ltd., London, UK).

Acknowledgments: The authors would like to thank Pilkington Glass, UK for the supply of substrates and Aleka Manousaki for the help with the SEM characterization.

Conflicts of Interest: The authors declare no conflict of interest.

References

1. Drosos, C.; Vernardou, D. Perspectives of energy materials by APCVD. *Sol. Energy Mater. Sol. C* **2015**, *140*, 1–4. [[CrossRef](#)]
2. Chen, X.; Wang, X.; Wang, Z.; Wan, J.; Liu, J.; Qian, Y. An ethylene glycol reduction approach to metastable VO₂ nanowire arrays. *Nanotechnology* **2004**, *15*, 1685–1687. [[CrossRef](#)]
3. Graf, D.; Schläfer, J.; Garbe, S.; Klein, A.; Mathur, S. Interdependence of structure, morphology and phase transitions in CVD grown VO₂ and V₂O₃ nanostructures. *Chem. Mater.* **2017**, *29*, 5877–5885. [[CrossRef](#)]

4. Wang, S.; Liu, M.; Kong, L.; Long, Y.; Jiang, X.; Yu, A. Recent progress in VO₂ smart coatings: Strategies to improve the thermochromic properties. *Prog. Mater. Sci.* **2016**, *81*, 1–54. [[CrossRef](#)]
5. Joushaghani, A.; Jeong, J.; Paradis, S.; Alain, D.; Aitchison, J.S.; Poon, J.K.S. Wavelength-size hybrid Si-VO₂ waveguide electroabsorption optical switches and photodetectors. *Opt. Express* **2015**, *23*, 3657–3688. [[CrossRef](#)] [[PubMed](#)]
6. Driscoll, T.; Kim, H.-T.; Chae, B.-G.; Ventra, M.D.; Basov, D.N. Phase-transition driven memristive system. *Appl. Phys. Lett.* **2009**, *95*, 043503. [[CrossRef](#)]
7. Pickett, M.D.; Medeiros-Ribeiro, G.; Williams, R.S. A scalable neuristor built with Mott memristors. *Nat. Mater.* **2013**, *12*, 114–117. [[CrossRef](#)] [[PubMed](#)]
8. Zhou, Y.; Ramanathan, S. Memory and neuromorphic devices. *Proc. IEEE* **2015**, *103*, 1289–1310. [[CrossRef](#)]
9. Louloudakis, D.; Vernardou, D.; Spanakis, E.; Suche, M.; Kenanakis, G.; Pemble, M.E.; Savvakis, C.; Katsarakis, N.; Koudoumas, E.; Kiriakidis, G. Atmospheric pressure chemical vapour deposition of amorphous tungsten doped vanadium dioxide for smart window applications. *Adv. Mater. Lett.* **2016**, *7*, 192–196. [[CrossRef](#)]
10. Vernardou, D.; Louloudakis, D.; Spanakis, E.; Katsarakis, N.; Koudoumas, E. Amorphous thermochromic VO₂ coatings grown by APCVD at low temperatures. *Adv. Mater. Lett.* **2015**, *6*, 660–663. [[CrossRef](#)]
11. Morrison, V.R.; Chatelain, R.P.; Tiwari, K.L.; Hendaoui, A.; Bruhács, A.; Chaker, M.; Siwick, B.J. A photoinduced metal-like phase of monoclinic VO₂ revealed by ultrafast electron diffraction. *Science* **2014**, *346*, 445–448. [[CrossRef](#)] [[PubMed](#)]
12. Eyert, V. The metal-insulator transition of VO₂: A band theoretical approach. *Ann. Phys.* **2002**, *11*, 650–704. [[CrossRef](#)]
13. Warwick, M.E.A.; Binions, R. Advances in thermochromic vanadium dioxide films. *J. Mater. Chem. A* **2014**, *2*, 3275–3292. [[CrossRef](#)]
14. Goodenough, J.B. The two components of the crystallographic transition in VO₂. *J. Solid State Chem.* **1971**, *3*, 490–500. [[CrossRef](#)]
15. Wentzcovitch, R.M.; Schulz, W.W.; Allen, P.B. VO₂: Peierls or Mott-Hubbard? A view from band theory. *Phys. Rev. Lett.* **1994**, *72*, 3389–3392. [[CrossRef](#)] [[PubMed](#)]
16. Maruyama, T.; Ikuta, Y. Vanadium dioxide thin films prepared by chemical vapour deposition from vanadium(III) acetylacetonate. *J. Mater. Sci.* **1993**, *28*, 5073–5078. [[CrossRef](#)]
17. Louloudakis, D.; Vernardou, D.; Spanakis, E.; Katsarakis, N.; Koudoumas, E. Thermochromic vanadium oxide coatings grown by APCVD at low temperatures. *Phys. Procedia* **2013**, *46*, 137–141. [[CrossRef](#)]
18. Vernardou, D.; Louloudakis, D.; Spanakis, E.; Katsarakis, N.; Koudoumas, E. Thermochromic amorphous VO₂ coatings grown by APCVD using a single-precursor. *Sol. Energy Mater. Sol. C* **2014**, *128*, 36–40. [[CrossRef](#)]
19. Vernardou, D.; Bei, A.; Louloudakis, D.; Katsarakis, N.; Koudoumas, E. Oxygen source-oriented control of atmospheric pressure chemical vapour deposition of VO₂ for capacitive applications. *J. Electrochem. Sci. Eng.* **2016**, *6*, 165–173. [[CrossRef](#)]
20. Louloudakis, D.; Vernardou, D.; Spanakis, E.; Dokianakis, S.; Panagopoulou, M.; Raptis, G.; Aperathitis, E.; Kiriakidis, G.; Katsarakis, N.; Koudoumas, E. Effect of O₂ flow rate on the thermochromic performance of VO₂ coatings grown by atmospheric pressure CVD. *Phys. Status Solidi C* **2015**, *12*, 856–860. [[CrossRef](#)]
21. Vernardou, D.; Louloudakis, D.; Spanakis, E.; Katsarakis, N.; Koudoumas, E. Functional properties of APCVD VO₂ layers. *Int. J. Thin Films Sci. Technol.* **2015**, *4*, 187–191. [[CrossRef](#)]
22. Vernardou, D.; Apostolopoulou, M.; Louloudakis, D.; Katsarakis, N.; Koudoumas, E. Electrochemical performance of vanadium oxide coatings grown using atmospheric pressure CVD. *Chem. Vap. Depos.* **2015**, *21*, 369–374. [[CrossRef](#)]
23. Zhang, Z.; Gao, Y.; Luo, H.; Kang, L.; Chen, Z.; Du, J.; Kanehira, M.; Zhang, Y.; Wang, Z.L. Solution-based fabrication of vanadium dioxide on F:SnO₂ substrates with largely enhanced thermochromism and low-emissivity for energy-saving applications. *Energy Environ. Sci.* **2011**, *4*, 4290–4297. [[CrossRef](#)]
24. Vernardou, D.; Pemble, M.E.; Sheel, D.W. The growth of thermochromic VO₂ films on glass by atmospheric-pressure CVD: A comparative study of precursors, CVD methodology and substrates. *Chem. Vap. Depos.* **2006**, *12*, 263–274. [[CrossRef](#)]
25. Bêteille, F.; Mazerolles, L.; Livage, J. Microstructure and metal-insulating transition of VO₂ thin films. *Mater. Res. Bull.* **1999**, *34*, 2177–2184. [[CrossRef](#)]

26. Malarde, D.; Powell, M.J.; Quesada-Cabrera, R.; Wilson, R.L.; Carmalt, C.J.; Samkar, G.; Parkin, I.P.; Palgrave, R.G. Optimized atmospheric-pressure chemical vapour deposition thermochromic VO₂ thin films for intelligent window applications. *ACS Omega* **2017**, *2*, 1040–1046. [[CrossRef](#)]
27. Powell, M.J.; Godfrey, I.J.; Quesada-Cabrera, R.; Malarde, D.; Teixeira, D.; Emerich, H.; Palgrave, R.G.; Carmalt, C.J.; Parkin, I.P.; Sankar, G. Qualitative XANES and XPS analysis of substrate effects in VO₂ thin films: A route to improving chemical vapour deposition synthetic methods? *J. Phys. Chem. C* **2017**, *121*, 20345–20352. [[CrossRef](#)]
28. Powell, M.J.; Quesada-Cabrera, R.; Taylor, A.; Teixeira, D.; Papakonstantinou, I.; Palgrave, R.G.; Sankara, G.; Parkin, I.P. Intelligent multifunctional VO₂/SiO₂/TiO₂ coatings for self-cleaning, energy-saving window panels. *Chem. Mater.* **2016**, *28*, 1369–1376. [[CrossRef](#)]



© 2018 by the authors. Licensee MDPI, Basel, Switzerland. This article is an open access article distributed under the terms and conditions of the Creative Commons Attribution (CC BY) license (<http://creativecommons.org/licenses/by/4.0/>).